HHS Public Access

Author manuscript

Cell Rep. Author manuscript; available in PMC 2016 November 10.

Published in final edited form as:

Cell Rep. 2016 October 4; 17(2): 570–582. doi:10.1016/j.celrep.2016.09.029.

Cytosolic accumulation of L-proline disrupts GABA-ergic transmission through GAD blockade

Gregg W Crabtree[1], **Alan J Park**[2], **Joshua A Gordon**[2,3], and **Joseph A Gogos**[1,4]

Joshua A Gordon: jag90@cumc.columbia.edu

[1]Department of Physiology and Cellular Biophysics, Columbia University Medical Center, New York, NY 10032, USA

[2]Department of Psychiatry, Columbia University, New York, NY 10032, USA

[3]Division of Integrative Neuroscience, New York State Psychiatric Institute, New York, NY 10032, USA

[4]Department of Neuroscience, Columbia University Medical Center, New York, NY 10032, USA

SUMMARY

Proline dehydrogenase (PRODH), which degrades L-proline, resides within the schizophrenia-linked 22q11.2 deletion suggesting a role in disease. Supporting this, elevated L-proline levels have been shown to increase risk for psychotic disorders. Despite the strength of data linking *PRODH* and L-proline to neuropsychiatric diseases, targets of disease-relevant concentrations of L-proline have not been convincingly described. Here we show that *Prodh*-deficient mice with elevated CNS L-proline display specific deficits in high-frequency GABA-ergic transmission and gamma-band oscillations. We find that L-proline is a GABA-mimetic and can act at multiple GABA-ergic targets. However, at disease-relevant concentrations, GABA-mimesis is limited to competitive blockade of glutamate decarboxylase leading to reduced GABA production. Significantly, deficits in GABA-ergic transmission are reversed by enhancing net GABA production with the clinically-relevant compound vigabatrin. These findings indicate that accumulation of a neuroactive metabolite can lead to molecular and synaptic dysfunction and help to understand mechanisms underlying neuropsychiatric disease.

Graphical Abstract

Correspondence: Joseph A Gogos (jag90@cumc.columbia.edu) or Gregg W Crabtree (gwc2@columbia.edu).

AUTHOR CONTRIBUTIONS

G.W.C, A.J.P., J.A. Gordon, and J.A.G. designed experiments, interpreted findings, and wrote the manuscript. G.W.C. and A.J.P. executed experiments and analyzed experimental data. J.A. Gordon and J.A.G. supervised the work.

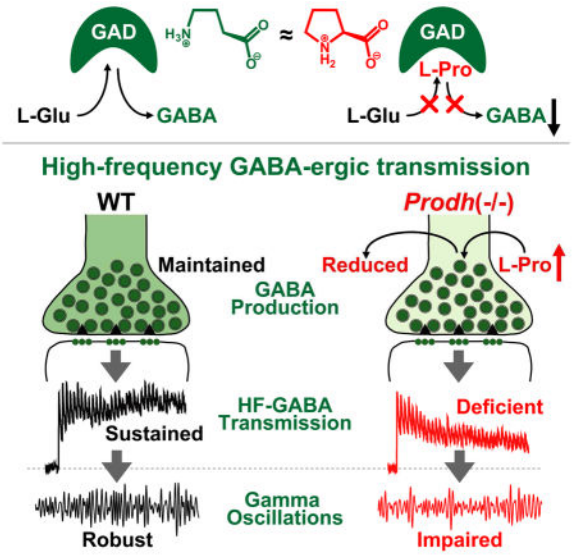

INTRODUCTION

There are a large number of relatively rare human diseases in which genetic mutations result in dysfunction of distinct enzymes embedded within metabolic networks, leading in turn to the pathological accumulation of specific metabolites. A subset of these diseases also manifests neuropsychiatric dysfunction (Rahman et al., 2013; Nia, 2014). Evidence supporting detailed mechanisms by which these accumulated small-molecule metabolites directly cause neuropsychiatric manifestations, however, has rarely been convincingly described (Rahman et al., 2013; Nia 2014). That both clinical pharmaceuticals and drugs of abuse can acutely cause psychosis in otherwise normal individuals suggests the possibility that pathological accumulation of certain endogenous small-molecule metabolites might likewise contribute to psychosis. Although the potential role of derangements of such metabolites in the pathogenesis of psychosis and other neuropsychiatric phenotypes remains understudied, recent metabolomic profiling in schizophrenia cohorts has suggested a potential contribution of variations of distinct metabolites in this disease (Yang et al., 2013; Clelland et al., 2011; Tomiya et al., 2007).

One metabolite accumulation within the CNS in neuropsychiatric diseases that may play a causal role in psychosis is the accumulation of L-proline due to deletion or dysfunction of *PRODH* (L-proline dehydrogenase). Individuals with isolated deletions or deleterious missense mutations in this gene, or larger encompassing deletions in the context of 22q11.2 deletion syndrome (22q11.2-DS) demonstrate L-proline elevations and increased risk for psychotic disorders (Clelland et al., 2011; Raux et al., 2007; Vorstman et al., 2009; Willis et al., 2008; Jacquet et al., 2005). Significantly, the severity of hyperprolinemia in patients correlates with the risk of psychosis and clinical severity (Raux et al., 2007; Clelland et al., 2011). A substantial body of clinical data supports that elevated CNS L-proline may cause neuronal dysfunction by interfering with native neurotransmitter systems (Willis et al., 2008). In this regard, we noted the chemical structure of L-proline closely resembles that of GABA, suggesting pathological levels of L-proline might specifically disrupt normal

GABA-ergic function. Here we provide multiple lines of evidence that L-proline acts as a GABA-analogue and that in hyperprolinemic disease competitive inhibition of GAD by elevated cytosolic L-proline leads to selective dysfunction in high-frequency GABA-ergic transmission. Consistent with deficits in high-frequency GABA-ergic drive, *in vivo* evaluation of network performance revealed specific and robust deficits in gamma oscillations. Our results highlight a unique mechanism of neuronal dysfunction in psychiatric disorders whereby cytosolic accumulation of a neuroactive metabolite disrupts neurotransmitter synthesis leading to a specific synaptic dysfunction. This finding raises the possibility of a potentially broader, important contribution of both GABA-mimetic and other neuroactive metabolites in accounting in part for the large genetic and neural heterogeneity of neuropsychiatric disease (Rodriguez-Murillo et al., 2012).

RESULTS

Isolated deficits in sustained GABA release in mice with elevated CNS L-proline

To look for possible alterations in evoked synaptic transmission caused by L-proline accumulation within the CNS, we performed patch clamp recordings from layer II/III pyramidal neurons of the medial prefrontal cortex (mPFC) in acute brain slices prepared from 4 to 6 week old hyperprolinemic *Prodh*(−/−) mice and WT littermates (Gogos et al., 1999). We chose to examine evoked synaptic transmission at layer II-III pyramidal neurons as action potential-mediated neurotransmission between neurons within this layer is believed to be critically involved in local network computations in the PFC, a brain region that has been strongly implicated in the pathophysiology of schizophrenia and psychosis (Uhlhaas and Singer, 2010; Bartos et al., 2007).

We assessed electrically evoked GABA-ergic synaptic transmission at layer II/III pyramidal cells by stimulating in layer II near the boundary between layer I and layer II, approximately 75–150μm from the soma of the recorded pyramidal neuron and performing whole-cell voltage-clamp recordings at 0mV in the presence of CNQX (10μM) and d-APV (50μM) to ensure isolation of monosynaptic GABA-ergic transmission. Baseline GABA-ergic transmission (single-stimulus evoked IPSCs) was unaltered in *Prodh*(−/−) mice (Figure S1A). We also evaluated short-term synaptic plasticity with a paired-pulse stimulation paradigm employing inter-stimulus intervals ranging from 25msec to 1sec. We found that paired-pulse ratios of the amplitudes of IPSCs were not significantly different between genotypes (Figures 1A, 1B; $p > 0.05$ at all inter-stimulus intervals, unpaired t-test) indicating that the presynaptic probability of GABA release was unaltered in *Prodh*(−/−) mice. Upon assessing depression of the amplitude of IPSCs during physiologically relevant stimulus trains, however, we found significantly increased synaptic depression in *Prodh*(−/−) mice at both 10Hz and 33Hz (Figures 1C, 1D, S2A, S2B; 10Hz: $p = 0.042$; 33Hz: $p = 0.038$, 2-way RM ANOVA), suggesting the possibility of presynaptic depletion of GABA (Zucker and Regehr, 2002).

We then examined whether synaptic alterations were confined to GABA-ergic transmission in hyperprolinemic mice. We assessed evoked glutamatergic transmission with whole-cell voltage-clamp recordings at −70mV – close to the GABA-A receptor reversal potential – to isolate glutamatergic transmission. Baseline transmission (single-stimulus evoked EPSCs)

was unaltered (Figure S1B). Similar to GABA-ergic transmission, we also found that paired-pulse ratios of the amplitudes of EPSCs were not significantly different between genotypes (Figures 1E, 1F; $p > 0.05$ at all inter-stimulus intervals, unpaired t-test) indicating that the presynaptic probability of glutamate release was likewise unaltered in *Prodh*(−/−) mice. In contrast to GABA-ergic transmission, however, we found that the depression of the amplitude of the EPSCs during stimulus trains was not significantly different between genotypes (Figures 1G, 1H, S2C, S2D; 10Hz: $p = 0.73$; 33Hz: $p = 0.96$, 2-way RM ANOVA) suggesting that presynaptic depletion of releasable glutamate during trains was unaltered in *Prodh*(−/−) mice. In summary, while evoked synaptic transmission was largely normal at layer II/III pyramidal neurons in the mPFC of *Prodh*(−/−) mice, these mice displayed a specific deficit in sustained, high-frequency GABA-ergic synaptic transmission as evidenced by increased synaptic depression.

L-proline is a structural homologue of GABA and is GABA-mimetic

We noted that the chemical structure of L-proline closely resembles that of GABA (Figure 2A) and this similarity might underlie the GABA-ergic specificity of synaptic dysfunction observed in *Prodh*(−/−) mice. We first explored the possibility that L-proline might neuroactively interfere with GABA-A or GABA-B receptor function and lead to the synaptic alterations we observed. While direct measures of extracellular L-proline levels in the brains of patients with hyperprolinemia are lacking, indirect measures strongly suggest that L-proline levels are very unlikely to exceed 30μM in this extracellular compartment (Phang et al., 2001). Employing whole-cell voltage clamp recordings from HEK-293 cells heterologously expressing GABA-A receptors we found that while high, millimolar concentrations of L-proline could activate GABA-A receptors (Figures 2B–2D: EC_{50}: 8.3mM, α1β1γ2; 5.4mM, α5β1γ2), even 100μM L-proline – a concentration exceeding pathophysiologically relevant extracellular CNS L-proline levels – could not detectably act at these channels. Furthermore, even millimolar concentrations of L-proline only weakly activated GABA-A receptors at normal resting membrane potentials (e.g., −70mV, Figure 2B), with L-proline-evoked activation being strongly favored at significantly depolarized potentials (Pavlov et al., 2009)(Figure 2B). Qualitatively similar results obtained from parallel whole-cell recordings in cultured cortical neurons confirmed these findings (data not shown). Consistent with our findings in cultured neurons, recordings in layer II/III pyramidal neurons revealed no evidence suggesting significantly altered tonic activation of GABA-A receptor currents as both input resistance and resting membrane potential of these neurons were unaltered in *Prodh*(−/−) mice (Figure S3). Recordings assessing GABA-B receptor combinations heterologously co-expressed with a G protein-coupled inwardly-rectifying potassium channel similarly revealed that while 10mM L-proline could robustly activate GABA-B receptors (Figures 2E, 2F), disease-relevant extracellular CNS concentrations did not evoke detectable GABA-B mediated responses (Figure 2F). Taken together results obtained at disease relevant extracellular L-proline concentrations strongly argue against GABA-A or GABA-B receptors as pathophysiologically relevant targets of L-proline in human disease.

To better localize the site of L-proline-mediated dysfunction we carried out additional assessments of GABA-ergic function. Immunohistochemistry in WT mouse mPFC showed

that PRODH is normally widely expressed in neurons, including PV+ GABA-ergic neurons (Figures 3A, 3B, S4A, S4B). Although there were no marked alterations in either the number or distribution of either GAD67+ or parvalbumin positive (PV+) interneurons in prelimbic mPFC in *Prodh*(−/−) mice (data not shown), localization of PRODH in GABA-ergic interneurons – including PV+ interneurons – suggests that PRODH dysfunction and L-proline accumulation could directly impact interneuron function. Indeed our initial synaptic findings were strongly suggestive of a presynaptic mechanism involving enhanced depletion of releasable GABA in *Prodh*(−/−) mice (Figures 1C, 1D, S1A, S2A, S2B). Therefore, we assessed this possibility further. Although accelerated IPSC decay kinetics could cause reduced synaptic summation leading to an observation of enhanced synaptic depression similar to that observed in *Prodh*(−/−) mice, comparison of IPSC decay rates during stimulus trains revealed no differences between genotypes further indicating that postsynaptic GABA receptor function is largely unaltered in hyperprolinemic mice, thus ruling out this potential post-synaptic mechanism (Figures 3C, 3D; IPSC decay rate, 10Hz: $p = 0.51$; 33Hz: $p = 0.15$, 2-way RM ANOVA). We next indirectly probed presynaptic function further to determine whether observed deficits in sustained GABA-ergic transmission might be due to a deficit in releasable GABA in *Prodh*(−/−) mice. Enhancement of extracellular accumulation of synaptically released GABA through GAT-1 blockade (NNC-711, 10μM) revealed markedly reduced and delayed summation of IPSCs during high-frequency (33Hz) stimulus trains in *Prodh*(−/−) mice compared to WT mice consistent with a deficit in presynaptic GABA under conditions of high-demand release (Figures 3E–3G; Maximal response, $p = 0.042$; Latency, $p = 0.018$, unpaired t-test). Taken together, the results of synaptic experiments argue strongly that *Prodh*(−/−) mice have a specific deficit in presynaptic GABA release under conditions of high-demand synaptic release (Figures 1, S1, S2, 3C–G).

We next considered potential physiologically relevant *in vivo* consequences arising from the deficits in high-frequency sustained GABA-ergic transmission we observed *in vitro*. A number of studies have suggested that sustained high frequency GABA-ergic drive arising from fast spiking PV+ interneurons is responsible for the generation of gamma oscillations (Cardin et al., 2009, Sohal et al., 2009; Bartos et al., 2007; Vreugdenhil et al., 2003). Because *Prodh*(−/−) mice showed specific deficits in GABA-ergic synaptic transmission during high-frequency stimulus trains and PRODH is expressed in PV-positive interneurons, we hypothesized that gamma oscillations would be impaired in *Prodh*(−/−) mice. We tested this hypothesis by recording local field potentials (LFPs) in mPFC of *Prodh*(−/−) mice and WT littermates during performance of a linear maze task (Fig. 4). We found a robust reduction in 30–80 Hz gamma power in *Prodh*(−/−) mice (Figure 4A, 4C, 4D; mean normalized power, WT: 2.0 ± 0.1, *Prodh*(−/−): 1.4 ± 0.1; Wilcoxon rank-sum test, $p = 0.000174$, Bonferroni-corrected). Low frequency power was not significantly affected (Figure 4B–4D; mean 1–4 Hz power, WT: 110.3 ± 9.6, *Prodh*(−/−): 117.3 ± 3.4, $p = 0.14$; mean 4–12 Hz power, WT: 32.5 ± 2.4, *Prodh*(−/−): 35.8 ± 2.1, $p = 0.21$;mean 12–30 Hz power, WT: 20.5 ± 1.4, *Prodh*(−/−): 19 ± 0.5, $p = 0.76$, Bonferroni-corrected). Interestingly, in concordance with our *in vitro* finding that *Prodh*(−/−) mice displayed enhanced synaptic depression in response to 33 Hz stimulation, these mice showed the most profound power deficits at ~38 Hz (Figure 4C). Taken together with *in vitro* findings, these *in vivo* findings provide evidence consistent with the deficit in high-frequency GABA-ergic transmission

observed *in vitro* in *Prodh*(−/−) mice as a likely contributing factor to the deficits in gamma oscillations observed *in vivo*. Collectively, these findings provide both *in vitro* and *in vivo* evidence for an important role for processes downstream of the *Prodh* gene in the generation of high-frequency neural activity. Further, given the important role gamma oscillations play in organizing local network activity during cognitive tasks (Roux and Uhlhaas, 2014; Uhlhaas and Singer, 2010; Chen et al., 2014), these findings strongly suggest that deficits in high-frequency GABA-ergic transmission could contribute to cognitive deficits both in patients with isolated hyperprolinemia and in the large fraction of 22q11-DS patients that also present with hyperprolinemia. (Raux et al., 2007; Clelland et al., 2011; Willis et al., 2008; Jacquet et al., 2005; Kempf et al., 2008; Jacquet et al., 2002; Li et al., 2008; Roussos et al., 2009).

Cytosolic L-proline elevations impair GABA production and synaptic transmission due to GAD blockade

We next sought to determine the mechanism of L-proline mediated presynaptic dysfunction that led to the deficits in sustained GABA-ergic transmission. Although our results indicated that GABA-A and GABA-B receptors were not credible targets of L-proline at disease relevant concentrations (Figures 2B–F, S3), activation of these GABA receptors with millimolar levels of L-proline indicated that L-proline is GABA-mimetic and suggested it could potentially interfere with other GABA-ergic targets regulating synaptic function. We also noted that the vast majority of small molecule metabolites – including L-proline – are normally preferentially confined (typically with a 10–100 fold enrichment) to the intracellular compartment as opposed to the extracellular space (Bennett et al., 2008, 2009). Furthermore previous studies indicating a normal level of ~1mM total free brain L-proline increasing to ~5–6mM in *Prodh*(−/−) mice in the context of low micromolar levels of extracellular CNS L-proline indicated that the majority of L-proline accumulation in the cerebral cortex of *Prodh*(−/−) mice must likewise be preferentially confined to the intracellular compartment and at concentrations close to 5mM (Gogos et al., 1999). Given our evidence of L-proline GABA-mimesis (Figure 2) and the significant structural homology between L-proline and GABA (Figure 2A), we considered possible intracellular GABA-ergic targets of L-proline that could account for the apparent selective reduction in presynaptic releasable GABA in the PFC of *Prodh*(−/−) mice.

We hypothesized that elevated cytosolic L-proline in *Prodh*(−/−) GABA-ergic neurons might reduce GABA synthesis through competitive inhibition of glutamate decarboxylase (GAD). In support of this hypothesis, we noted the enhanced synaptic depression of GABA-ergic responses during stimulus trains we observed in *Prodh*(−/−) mice was remarkably reminiscent of the enhanced GABA-ergic synaptic depression during stimulus trains that was the most prominent synaptic dysfunction in *Gad65*(−/−) mice (Tian et al., 1999).

To test whether L-proline inhibited GAD synthesis of GABA, we performed *in vitro* assays of GABA production utilizing both heterologously expressed human GAD67 as well as GAD isolated from a mouse PFC cytosolic fraction. For these assays cytosolic L-proline concentrations were inferred from previous measures of whole brain (wet brain tissue) L-proline in both WT and *Prodh*(−/−) mice (Gogos et al., 1999). As intracellular volume is the

dominant contribution to brain volume (far exceeding extracellular space in which L-proline unlikely exceeds 30μMin mutant mice, Gogos et al., 1999; Phang et al., 2001), these inferred values of ~5–6mM cytosolic L-proline levels (compared to a normal cytosolic L-proline concentration of ~1mM) represent conservative estimates of neuronal cytosolic L-proline concentrations.

In vitro GAD activity reactions were incubated at 37°C for 1hr and employed physiological levels of L-glutamate (5mM) as substrate and either normal (1mM) or hyperprolinemic levels (5mM) of cytosolic L-proline (Gogos et al. 1999). HPLC analysis of the reaction products of these assays showed that reactions that included 5mM L-proline had reduced GABA synthesis by approximately 25% compared to those that included 1mM L-proline (Figures 5A, 5B; hGAD67: $p = 4.3 \times 10^{-8}$; mouse PFC GAD fraction: $p = 0.013$, unpaired t-tests). A more comprehensive inhibition study further indicated that L-proline inhibition of GAD67 was competitive and characterized by a K_i of 7.8mM (Figure 5C). These results indicate that pathophysiological concentrations of L-proline can inhibit GAD-dependent synthesis of GABA and that such GAD blockade by elevated cytosolic L-proline in *Prodh*(−/−) mice may be responsible for the deficits in GABA-ergic synaptic transmission we observed during high-frequency stimulus trains (Figure 1, S2).

We next looked for more direct evidence that L-proline blockade of GAD-dependent GABA synthesis could be functionally significant and responsible for the enhanced depression in GABA-ergic synaptic transmission observed during high-frequency stimulus trains. To address this possibility we first tested whether acute pharmacological blockade of GAD in the mPFC of WT mice could phenotypically mimic the GABA release deficits observed in *Prodh*(−/−) mice. To mimic L-proline blockade of GAD in *Prodh*(−/−) mice, acute WT brain slices were pre-incubated with the competitive GAD antagonist 3-mercaptopropionic acid (3-MPA, 1mM) for 2 hours and postsynaptic GABA-ergic responses to 33Hz stimulus trains were then assessed in the continuous presence of 100μM 3-MPA. We found that the amplitude of the IPSCs during 33Hz stimulus trains showed significantly increased synaptic depression in WT brain slices treated with 3-MPA compared to those in untreated WT slices (Figures 5D, 5E; $p = 0.00090$, 2-way RM ANOVA). This result indicated that GAD blockade leads to enhanced synaptic depression similar to that observed in *Prodh*(−/−) mice.

Furthermore, in contrast to findings in WT, GAD blockade with 3-MPA in *Prodh*(−/−) brain slices did not lead to further increases in synaptic depression of IPSCs during 33Hz stimulus trains (Figure 5E; $p = 0.87$, 2-way RM ANOVA) consistent with a near-maximal impact of basal GAD-blockade upon GABA-ergic transmission in *Prodh*(−/−) mice. This result further suggests that the observed partially sustained high-frequency GABA-ergic responses (Figures 1C, 1D, 5E–5G) are likely due to emergence of predominantly GAD-independent, GABA-conserving compensatory mechanisms. A trend towards elevated GAD activity in PFC cytosolic fractions isolated from *Prodh*(−/−) mice (Figure S5, $p = 0.12$, unpaired t-test) additionally suggested the possibility that *in vivo* blockade of GAD in *Prodh*(−/−) mice may trigger a compensatory upregulation of GAD expression. This finding suggests that the enhanced short-term depression observed in *Prodh*(−/−) mice is not due to reduced expression of GAD isoforms.

Importantly we also assessed whether enhancing net GABA production reverses the deficits in sustained GABA-release. In parallel experiments employing an identical stimulus paradigm, enhancing net GABA production in *Prodh*(−/−) mice with the irreversible GABA-transaminase inhibitor vigabatrin (1500mg/kg, IP injection 2.5 days prior to recording; Gale and Iadarola, 1980) led to the near elimination of the enhanced synaptic depression in response to 33Hz stimulus trains seen in untreated (Figure 1) or vehicle-treated *Prodh*(−/−) mice (Figures 5F, 5G; p = 0.041, 2-way RM ANOVA; no effect on short-term plasticity during the first 5 responses, p = 0.13, 2-way RM ANOVA).

These results obtained with pharmacological manipulations of GABA production in brain slices support that the enhanced GABA-ergic synaptic depression during sustained high-frequency stimulation results from a deficit in GABA production in *Prodh*(−/−) mice. In concert with *in vitro* results showing L-proline blockade of GAD (Figure 5A–C), these results strongly support the notion that this enhanced GABA-ergic synaptic depression arises due to deficits in GABA production resulting from significant *in vivo* blockade of GAD by L-proline accumulated within the cytosol of inhibitory neurons.

DISCUSSION

Our findings suggest a mechanism of neuronal dysfunction potentially important in the pathogenesis of schizophrenia and other neuropsychiatric disorders whereby accumulation of an endogenous neuroactive metabolite in disease leads to severe and specific deficits in synaptic function and neural circuit performance. Specifically, our results show that L-proline is a GABA-analogue, and that L-proline accumulation in the cytosol of GABA-ergic neurons causes competitive inhibition of GAD leading to deficient GABA production. This results in a specific functional impact limited to deficits in sustained, high-frequency GABA-ergic transmission, a high synaptic demand condition under which GABA production via GAD is critical to maintaining ongoing transmission (Hajos et al., 2004; Bartos et al., 2007; Hefft and Jonas, 2005; Tian et al., 1999; Wang et al., 2013). Similarly circumscribed deficits have been previously described in GAD65-null mice (Tian et al., 1999). By contrast, lower GABA-demand conditions such as baseline transmission (single stimulus) and very short-term plasticity (paired-pulse ratio) are unchanged, as was similarly observed in GAD65-null mice (Tian et al., 1999).

During sustained GABA-ergic transmission GABA released from presynaptic terminals must be replenished either by *de novo* GABA synthesis via GAD or by GABA reuptake from the extracellular space (principally mediated by GAT-1) as GABA diffusion from adjacent cellular compartments is insufficient (Wang et al., 2013). While in principal both mechanisms could replenish GABA during sustained transmission, reuptake of GABA via GAT-1 does not appear critical while *de novo* synthesis by GAD is indispensible (Bragina et al., 2008; Wang et al., 2013; Tian et al., 1999). As such, blockade of GAD activity by elevated cytosolic L-proline – which similar to most small molecule metabolites is preferentially sequestered intracellularly (Bennett et al., 2008, 2009; Gogos et al., 1999) – would be expected to interfere with sustained GABA-ergic transmission (Tian et al., 1999; Wang et al, 2013). How GAD hypofunction and acute GABA depletion exactly lead to enhanced synaptic depression remains unknown (Tian et al., 1999; Wang et al, 2013) but

mechanisms including kiss-and-run recycling (Stevens and Williams, 2000; Alabi and Tsien, 2013) and rapid endocytosis (Pyle et al., 2000; Cárdenas and Marengo, 2010) may be involved. Both mechanisms lead to GABA release and vesicle refilling within the time course of our depression paradigms and would likely be sensitive to acute deficiencies in synaptic GABA production.

The reduced and delayed summation of GABA-ergic events in *Prodh*(−/−) mice observed during GAT-1 blockade compared to robust summation in WT mice also supports a deficit in sustained availability of presynaptic GABA during high-demand release in *Prodh*(−/−) mice (Tian et al., 1999). Further, acute blockade of GAD in WT mice led to deficits in sustained release similar to *Prodh*(−/−) mice while enhancing GABA content through blockade of GABA degradation with vigabatrin significantly rescued sustained GABA-ergic transmission. Notably, while high concentrations of L-proline could robustly activate both GABA-A and GABA-B receptors – confirming L-proline as a *bone fide* GABA analogue – this activation was only observed at supra-physiological concentrations far exceeding extracellular levels found in disease (Phang et. al., 2001). These findings largely rule out postsynaptic GABA-A/GABA-B receptors as possible disease-relevant mediators of the effects of elevated L-proline. Our finding of unaltered decay kinetics of GABA-ergic synaptic events further supported this conclusion, again pointing to a presynaptic alteration underlying the sustained GABA-ergic transmission deficit consistent with neurotransmitter depletion (Zucker and Regehr, 2002).

In addition to our results, the striking correspondence of our findings to the similarly circumscribed GABA-ergic deficits present in the GAD65-null mouse further supports our proposed mechanism of GAD hypofunction (Tian et al., 1999). While GABA-ergic transmission has not been assessed GAD67-null mice (due to non-viability), the specific deficiencies in sustained GABA release present in GAD65-null mice suggest that GAD65 could be a critical synaptic target of L-proline *in vivo*. GAD65 is preferentially localized to presynaptic terminals, is synaptic activity dependent, and is functionally coupled to vGAT and synaptic vesicles to facilitate vesicular GABA loading (Fenalti et al., 2007; Esclapez et al., 1994; Jin et al., 2003).

Our findings suggest L-proline's effect on inhibitory transmission is specific. We did not detect any alterations in evoked glutamatergic transmission – including during moderate to high frequency stimulus trains – consistent with the substantial shared structural homology of L-proline with GABA rather than with glutamate. However, we cannot exclude the possibility that reductions in GABA-ergic transmission due to L-proline may indirectly affect excitatory transmission and plasticity due to reductions in GABA-ergic modulatory influences (Guetg et al., 2009; Stell et al., 2007; Sakaba and Neher, 2003). Although we did not observe such effects, it is possible that such indirect effects could be revealed under different stimulation paradigms or in other brain areas.

Here we have assessed evoked synaptic transmission, which recapitulates the action potential-mediated neurotransmission responsible for driving moment-to-moment neural circuit computation. Whether L-proline accumulation also affects spontaneous synaptic activity (miniature synaptic events) remains to be determined. However, it is notable that

GAD hypofunction present in GAD65-null mice did not affect the frequency or amplitude of miniature synaptic events (Tian et al., 1999). Furthermore, our synaptic results showing GABA-ergic baseline transmission and very short term plasticity are both unchanged suggest that the synaptic impact of GAD blockade becomes functionally apparent only under high GABA demand scenarios (Tian et al., 1999).

With respect to possible functional outcomes due to GAD hypofunction, the sustained high-frequency GABA release that depends upon intact GAD function and *de novo* GABA synthesis (Wang et al., 2013; Tian et al., 1999; Fenalti et al., 2007; Esclapez et al., 1994; Jin et al., 2003; Bragina et al., 2008) may be most physiologically relevant for PV+ fast-spiking neurons in which high frequency action potentials are translated into high frequency GABA release (Hajos et al., 2004; Bartos et al., 2007; Hefft and Jonas, 2005; Szabó et al., 2010; Hu et al., 2014). In fact, the *in vivo* network alterations we found in *Prodh*(−/−) mice were consistent with deficits in sustained GABA-ergic transmission arising from PV+ interneurons.

The network dysfunction we observed that was limited specifically to robust deficits in gamma oscillations supports the relevance of the high-frequency GABA-ergic transmission deficits we observed *in vitro*. High-frequency GABA-ergic transmission from PV+ neurons onto layer II-III pyramidal neurons drives the generations of gamma oscillations critically involved in local network computations in the PFC and deficits in this drive are expected to lead to deficits in gamma oscillations (Bartos et al., 2007; Volman et al., 2011). Significantly, dysfunction of PFC gamma oscillations has been strongly implicated in the network pathophysiology underlying the cognitive deficits present schizophrenia (Uhlhaas and Singer, 2010; Chen et al., 2014). While the potential role of GAD hypofuction upon network function has not previously been described in GAD deficient mice, it is notable that models of cortical network function have predicted that GAD hypofuction leads to enhanced short term depression of GABA-ergic transmission and consequent reductions in the power of gamma oscillations, mirroring both our *in vitro* and *in vivo* findings (Volman et al., 2011).

Further, deficits in pre-pulse inhibition of acoustic startle and conditioned fear learning are shared as the most prominent behavioral findings in both *Prodh*(−/−) mice and GAD65-deficient mice (Heldt et al., 2004; Gogos et al., 1999; Stork et al., 2003; Paterlini et al., 2005) and both behaviors depend upon intact GAD function as well as upon PV+ interneuron function (Nguyen et al., 2014; Wolff et al., 2014). That deficits in sustained high frequency GABA release are the most prominent electrophysiological findings in both of these mutant mouse lines suggests their shared behavioral dysfunction might arise from shared deficits in sustained GABA release.

Elevation of L-proline levels in 22q11.2 deletion carriers is as an important component of the psychiatric risk associated with this genomic lesion and depends on the presence of hypomorphic *PRODH* alleles in the retained copy on the intact chromosome (Raux et al., 2007; Bender et al., 2005; Chakravarti, 2002; Liu et al., 2002; Willis et al., 2008; Zarchi et al., 2013). Significantly, the severity of hyperprolinemia in these patients correlates with risk of psychosis (Raux et al., 2007). Our findings illuminate mechanisms of L-proline-dependent dysfunction likely contributing to the psychiatric risk associated with 22q11.2

deletions and provide insights into GABA-ergic dysfunction emerging as a result of this genomic lesion. These findings also suggest straightforward approaches to targeted therapies that could be used to ameliorate or prevent GABA-ergic dysfunction. Additionally our results have broader implications for the genetic and neural mechanisms underlying psychosis.

First, reduced expression of both GAD67 and GAD65 have been repeatedly implicated in studies of schizophrenia cohorts suggesting that deficient sustained GABA release resulting from GAD hypofuction – such as observed both in GAD65-null mice as well as here in *Prodh*(−/−) mice – could significantly contribute to related disease dysfunction (Akbarian et al., 1995; Heckers et al., 2002; Benes et al., 2007; Rocco et al., 2015; Tian et al., 1999). Significantly, parallel studies have also commonly found reductions and alterations in PV+ interneurons (Hashimoto et al., 2003; Knable et al., 2004; Zhang and Reynolds, 2002). Further supporting a relevant pathological role, alterations in PV+ neurons have additionally been observed in diverse mouse models of schizophrenia (Fenelon et al., 2013; Niwa et al., 2010; Carlson et al., 2011; Del Pino et al., 2013; Wen et al., 2010). Functional alterations of PV+ neurons, which are uniquely designed for high-frequency, sustained GABA release (Hefft and Jonas, 2005; Szabó et al., 2010; Hu et al., 2014; Bartos et al., 2007; Hajos et al., 2004), may represent an important and relevant source of synaptic dysfunction in schizophrenia. Indeed, the fidelity of sustained GABA release from PV+ interneurons appears critical to network and behavioral dysfunction found in this disease (Constantinidis et al., 2002; Uhlhaas and Singer, 2010).

Second, studies have previously implicated elevated L-proline in susceptibility for schizophrenia and related disorders and showed severity of hyperprolinemia correlates with risk and severity of disease (Clelland et al., 2011; Willis et al., 2008; Jacquet et al., 2005; Kempf et al., 2008; Jacquet et al., 2002; Li et al., 2008; Roussos et al., 2009). Importantly, in addition to targeted studies that have implicated L-proline levels in schizophrenia risk (Clelland et al., 2011; Tomiya et al., 2007), a recent blind metabolomic study of schizophrenics, while not identifying L-proline itself, identified two metabolite risk candidates – 5-oxoproline and L-pipecolic acid – that bear striking structural homology to L-proline (Figure S6) (Yang et al., 2013; 2 out of the 22 total risk metabolites identified by this study). In this regard, it is further notable that L-pipecolic acid accumulates in pyridoxine dependent seizures – a disease long speculated to result from GAD hypofunction (Scriver and Whelan, 1969) – due to antiquitin deficiency and that 5-oxoproline accumulates in glutathione synthetase deficiency, a metabolic disease also associated with seizures and psychosis (Roberson et al., 1991). In the context of our results, these findings suggest the possibility of a broader and important contribution of both GABA-mimetic as well as other neuroactive metabolites in explaining in part the large genetic heterogeneity of neuropsychiatric disease (Rodriguez-Murillo et al., 2012). This also points towards the merit of exploring the potential of targeted and precise therapeutic interventions based on the genetic and metabolic profile of patients including reevaluation of the many clinically available pharmaceuticals know to enhance GABA-ergic function.

EXPERIMENTAL PROCEDURES

Animals

All animal procedures were carried out in accordance with and approved by the Columbia University Institutional Animal Care and Use Committee. Experiments were performed on homozygous *Prodh*-deficient male mice and their wild-type (WT) littermates. The generation of the *Prodh*(−/−) mice has been described previously (Paterlini et al., 2005).

Acute Brain Slice Electrophysiology

Medial prefrontal cortical slice preparation has been previously described (Fenelon et al., 2013). All mice were 4–6 wk old male littermates. All experiments employed whole-cell, voltage-clamp recordings from prelimbic and infralimbic mPFC layer II-III pyramidal neurons. Evoked synaptic responses were elicited with electric stimulation with a bipolar stimulating electrode positioned within layer II approximately 75 – 150 μm lateral from the recorded neuron. Neurons were held in voltage-clamp at −70mV to assess evoked excitatory synaptic responses and at 0mV in the presence of CNQX (10μM) and AP-V (50μM) to assess evoked inhibitory synaptic responses.

Recordings Employing Heterologously Expressed of GABA-A and GABA-B receptors

HEK-293 cells were transfected with indicated cDNA plasmids using Lipofectamine 2000 (Invitrogen) following the manufacturer's instructions. Transfected cells were used for voltage-clamp recordings 2–6 days after transfection.

In vivo Neurophysiology

Three to four months old *Prodh*(−/−) mice and WT littermates were anesthetized with isoflurane, placed in a stereotaxic apparatus, and implanted with a tungsten wire field electrode or a bundle of 15 tungsten wire stereotrodes in the mPFC. Wires were connected to a 16 or 36-channel electrode interface board (Neuralynx) fixed to the skull with dental cement. After surgical recovery, habituation, and task training in a linear track, local field potentials (LFPs) were recorded (Digital Lynx system) while mice were running in the linear track on two days, 20 min on each day. The multitaper method was used to compute power spectral density when running speed was 20–25 cm/s.

GAD activity assays

GAD fractions were obtained from either heterologous expression in BL21 E. coli or from mouse brain homogenates. GAD reactions were carried out at 37°C in GAD reaction buffer (100mM KPO_4, 1mM 2-aminoethylisothiouronium bromide (AET), and 100μM of pyridoxal-5′-phosphate, pH 7.2). L-glutamate was provided as substrate and L-proline was included in reactions to test for GAD inhibition. After quenching, reaction products were derivatized and assessed for GABA content via HPLC.

Statistical Analysis

For comparisons involving repeated measures, 2-way ANOVA repeated measures analyses were employed with Bonferroni post-hoc analysis. For all other simple comparisons

unpaired t-tests were employed that were two-sided except in cases in which there was a directional hypothesis. The mean power at different frequency bands was compared using Wilcoxon rank-sum test, with Bonferroni-corrected p-values for multiple comparisons.

A full description of these methodologies as well as for immunohistochemistry are provided in the Supplemental Experimental Procedures.

Supplementary Material

Refer to Web version on PubMed Central for supplementary material.

Acknowledgments

We thank Maria Karayiorgou for her support during earlier phases of this work. The authors also wish to thank Yan Sun, Caitlin Burgdorf, and Rachel Waldman for support with the maintenance of the mouse colony. Additionally, we thank Kimberly Stark and Natascha Diamantopoulou for oversight in the management of the mouse colony. We thank William Hardin and Alex Harris for assistance and advice with *in vivo* neurophysiology experiments. We also thank Liam Drew, Chiara Manzini, and Natascha Diamantopoulou for comments on the manuscript. Donald Landry provided generous access to his HPLC equipment in his laboratory. We thank Tom Cooper (Nathan Kline Institute) for additional support with HPLC analysis. This work was supported by NIH grants R21MH10069 and R01MH096274 (to JAG). The authors declare no competing financial interests.

References

Akbarian S, Kim JJ, Potkin SG, Hagman JO, Tafazzoli A, Bunney WE Jr, Jones EG. Gene expression for glutamic acid decarboxylase is reduced without loss of neurons in prefrontal cortex of schizophrenics. Arch Gen Psychiatry. 1995; 52:258–66. [PubMed: 7702443]

Alabi AA, Tsien RW. Perspectives on kiss-and-run: role in exocytosis, endocytosis, and neurotransmission. Annu Rev Physiol. 2013; 75:393–422. [PubMed: 23245563]

Bartos M, Vida I, Jonas P. Synaptic mechanisms of synchronized gamma oscillations in inhibitory interneuron networks. Nat Rev Neurosci. 2007; 8:45–56. [PubMed: 17180162]

Bender HU, Almashanu S, Steel G, Hu CA, Lin WW, Willis A, Pulver A, Valle D. Functional consequences of PRODH missense mutations. Am J Hum Genet. 2005; 76:409–20. [PubMed: 15662599]

Benes FM, Lim B, Matzilevich D, Walsh JP, Subburaju S, Minns M. Regulation of the GABA cell phenotype in hippocampus of schizophrenics and bipolars. Proc Natl Acad Sci USA. 2007; 104:10164–9. [PubMed: 17553960]

Bennett BD, Kimball EH, Gao M, Osterhout R, Van Dien SJ, Rabinowitz JD. Absolute metabolite concentrations and implied enzyme active site occupancy in Escherichia coli. Nat Chem Biol. 2009; 5:593–9. [PubMed: 19561621]

Bennett BD, Yuan J, Kimball EH, Rabinowitz JD. Absolute quantitation of intracellular metabolite concentrations by an isotope ratio-based approach. Nat Protoc 2008. 2008; 3:1299–311.

Bragina L, Marchionni I, Omrani A, Cozzi A, Pellegrini-Giampietro DE, Cherubini E, Conti F. GAT-1 regulates both tonic and phasic GABA(A) receptor-mediated inhibition in the cerebral cortex. J Neurochem. 2008; 105:1781–93. [PubMed: 18248614]

Cárdenas AM, Marengo FD. Rapid endocytosis and vesicle recycling in neuroendocrine cells. Cell Mol Neurobiol. 2010; 30:1365–70. [PubMed: 21046457]

Cardin JA, Carlén M, Meletis K, Knoblich U, Zhang F, Deisseroth K, Tsai LH, Moore CI. Driving fast-spiking cells induces gamma rhythm and controls sensory responses. Nature. 2009; 459:663–7. [PubMed: 19396156]

Carlson GC, Talbot K, Halene TB, Gandal MJ, Kazi HA, Schlosser L, Phung QH, Gur RE, Arnold SE, Siegel SJ. Dysbindin-1 mutant mice implicate reduced fast-phasic inhibition as a final common disease mechanism in schizophrenia. Proc Natl Acad Sci USA. 2011; 108:E962–70. [PubMed: 21969553]

Chakravarti A. A compelling genetic hypothesis for a complex disease: PRODH2/DGCR6 variation leads to schizophrenia susceptibility. Proc Natl Acad Sci U S A. 2002; 99:4755–6. [PubMed: 11959925]

Chen CM, Stanford AD, Mao X, Abi-Dargham A, Shungu DC, Lisanby SH, Schroeder CE, Kegeles LS. GABA level, gamma oscillation, and working memory performance in schizophrenia. Neuroimage Clin. 2014; 4:531–9. [PubMed: 24749063]

Clelland CL, Read LL, Baraldi AN, Bart CP, Pappas CA, Panek LJ, Nadrich RH, Clelland JD. Evidence for association of hyperprolinemia with schizophrenia and a measure of clinical outcome. Schizophr Res. 2011; 131:139–45. [PubMed: 21645996]

Constantinidis C, Williams GV, Goldman-Rakic PS. A role for inhibition in shaping the temporal flow of information in prefrontal cortex. Nat Neurosci. 2002; 5:175–80. [PubMed: 11802172]

Del Pino I, García-Frigola C, Dehorter N, Brotons-Mas JR, Alvarez-Salvado E, Martínez de Lagrán M, Ciceri G, Gabaldón MV, Moratal D, Dierssen M, et al. Erbb4 deletion from fast-spiking interneurons causes schizophrenia-like phenotypes. Neuron. 2013; 79:1152–68. [PubMed: 24050403]

Esclapez M, Tillakaratne NJ, Kaufman DL, Tobin AJ, Houser CR. Comparative localization of two forms of glutamic acid decarboxylase and their mRNAs in rat brain supports the concept of functional differences between the forms. J Neurosci. 1994; 14:1834–55. [PubMed: 8126575]

Fenalti G, Law RH, Buckle AM, Langendorf C, Tuck K, Rosado CJ, Faux NG, Mahmood K, Hampe CS, Banga JP, et al. GABA production by glutamic acid decarboxylase is regulated by a dynamic catalytic loop. Nat Struct Mol Biol. 2007; 14:280–6. [PubMed: 17384644]

Fénelon K, Xu B, Lai CS, Mukai J, Markx S, Stark KL, Hsu PK, Gan WB, Fischbach GD, MacDermott AB, et al. The pattern of cortical dysfunction in a mouse model of a schizophrenia-related microdeletion. J Neurosci. 2013; 33:14825–39. [PubMed: 24027283]

Gale K, Iadarola MJ. Seizure protection and increased nerve-terminal GABA: delayed effects of GABA transaminase inhibition. Science. 1980; 208:288–91. [PubMed: 6768130]

Gogos JA, Santha M, Takacs Z, Beck KD, Luine V, Lucas LR, Nadler JV, Karayiorgou M. The gene encoding proline dehydrogenase modulates sensorimotor gating in mice. Nat Genetics. 1999; 21:434–439. [PubMed: 10192398]

Guetg N, Seddik R, Vigot R, Turecek R, Gassmann M, Vogt KE, Bräuner-Osborne H, Shigemoto R, Kretz O, Frotscher M, et al. The GABAB1a isoform mediates heterosynaptic depression at hippocampal mossy fiber synapses. J Neurosci. 2009; 29:1414–23. [PubMed: 19193888]

Hájos N, Pálhalmi J, Mann EO, Németh B, Paulsen O, Freund TF. Spike timing of distinct types of GABAergic interneuron during hippocampal gamma oscillations in vitro. J Neurosci. 2004; 24:9127–37. [PubMed: 15483131]

Hashimoto T, Volk DW, Eggan SM, Mirnics K, Pierri JN, Sun Z, Sampson AR, Lewis DA. Gene expression deficits in a subclass of GABA neurons in the prefrontal cortex of subjects with schizophrenia. J Neurosci. 2003; 23:6315–26. [PubMed: 12867516]

Heckers S, Stone D, Walsh J, Shick J, Koul P, Benes FM. Differential hippocampal expression of glutamic acid decarboxylase 65 and 67 messenger RNA in bipolar disorder and schizophrenia. Arch Gen Psychiatry. 2002; 59:521–9. [PubMed: 12044194]

Hefft S, Jonas P. Asynchronous GABA release generates long-lasting inhibition at a hippocampal interneuron-principal neuron synapse. Nat Neurosci. 2005; 8:1319–28. [PubMed: 16158066]

Heldt SA, Green A, Ressler KJ. Prepulse inhibition deficits in GAD65 knockout mice and the effect of antipsychotic treatment. Neuropsychopharmacology. 2004; 29:1610–9. [PubMed: 15114343]

Hensch TK, Fagiolini M, Mataga N, Stryker MP, Baekkeskov S, Kash SF. Local GABA circuit control of experience-dependent plasticity in developing visual cortex. Science. 1998; 282:1504–8. [PubMed: 9822384]

Hu H, Gan J, Jonas P. Interneurons. Fast-spiking, parvalbumin^{+} GABAergic interneurons: from cellular design to microcircuit function. Science. 2014; 345:1255263. [PubMed: 25082707]

Jacquet H, Raux G, Thibaut F, Hecketsweiler B, Houy E, Demilly C, Haouzir S, Allio G, Fouldrin G, Drouin V, et al. PRODH mutations and hyperprolinemia in a subset of schizophrenic patients. Hum Mol Genet. 2002; 11:2243–9. [PubMed: 12217952]

Jacquet H, Demily C, Houy E, Hecketsweiler B, Bou J, Raux G, Lerond J, Allio G, Haouzir S, Tillaux A, et al. Hyperprolinemia is a risk factor for schizoaffective disorder. Mol Psychiatry. 2005; 10:479–85. [PubMed: 15494707]

Jin H, Wu H, Osterhaus G, Wei J, Davis K, Sha D, Floor E, Hsu CC, Kopke RD, Wu JY. Demonstration of functional coupling between gamma -aminobutyric acid (GABA) synthesis and vesicular GABA transport into synaptic vesicles. Proc Natl Acad Sci USA. 2003; 100:4293–8. [PubMed: 12634427]

Kahana MJ. The cognitive correlates of human brain oscillations. J Neurosci. 2006; 26:1669–72. [PubMed: 16467513]

Kash SF, Johnson RS, Tecott LH, Noebels JL, Mayfield RD, Hanahan D, Baekkeskov S. Epilepsy in mice deficient in the 65-kDa isoform of glutamic acid decarboxylase. Proc Natl Acad Sci U S A. 1997; 94:14060–5. [PubMed: 9391152]

Kempf L, Nicodemus KK, Kolachana B, Vakkalanka R, Verchinski BA, Egan MF, Straub RE, Mattay VA, Callicott JH, Weinberger DR, et al. Functional polymorphisms in PRODH are associated with risk and protection for schizophrenia and fronto-striatal structure and function. PLoS Genet. 2008; 4:e1000252. [PubMed: 18989458]

Knable MB, Barci BM, Webster MJ, Meador-Woodruff J, Torrey EF. Stanley Neuropathology Consortium. Molecular abnormalities of the hippocampus in severe psychiatric illness: postmortem findings from the Stanley Neuropathology Consortium. Mol Psychiatry. 2004; 9:609–20. [PubMed: 14708030]

Li T, Ma XH, Hu X, Wang YC, Yan CY, Meng HQ, Liu XH, Toulopoulou T, Murray RM, Collier DA. PRODH gene is associated with executive function in schizophrenic families. Am J Med Genet B. 2008; 147:654–7.

Liu H, Heath SC, Sobin C, Roos JL, Galke BL, Blundell ML, Lenane M, Robertson B, Wijsman EM, Rapoport JL, et al. Genetic variation at the 22q11 PRODH2/DGCR6 locus presents an unusual pattern and increases susceptibility to schizophrenia. Proc Natl Acad Sci U S A. 2002; 99:3717–22. [PubMed: 11891283]

Nguyen R, Morrissey MD, Mahadevan V, Cajanding JD, Woodin MA, Yeomans JS, Takehara-Nishiuchi K, Kim JC. Parvalbumin and GAD65 interneuron inhibition in the ventral hippocampus induces distinct behavioral deficits relevant to schizophrenia. J Neurosci. 2014; 34:14948–60. [PubMed: 25378161]

Nia S. Psychiatric signs and symptoms in treatable inborn errors of metabolism. J Neurol. 2014; 261:S559–68. [PubMed: 25145892]

Niwa M, Kamiya A, Murai R, Kubo K, Gruber AJ, Tomita K, Lu L, Tomisato S, Jaaro-Peled H, Seshadri S, et al. Knockdown of DISC1 by in utero gene transfer disturbs postnatal dopaminergic maturation in the frontal cortex and leads to adult behavioral deficits. Neuron. 2010; 65:480–9. [PubMed: 20188653]

Paterlini M, Zakharenko SS, Lai WS, Qin J, Zhang H, Mukai J, Westphal KG, Olivier B, Sulzer D, Pavlidis P, et al. Transcriptional and behavioral interaction between 22q11.2 orthologs modulates schizophrenia-related phenotypes in mice. Nat Neurosci. 2005; 8:1586–94. [PubMed: 16234811]

Pavlov I, Savtchenko LP, Kullmann DM, Semyanov A, Walker MC. Outwardly rectifying tonically active GABAA receptors in pyramidal cells modulate neuronal offset, not gain. J Neurosci. 2009; 29:15341–50. [PubMed: 19955387]

Phang, JM.; Hu, CA.; Valle, D. Disorders of proline and hydroxyproline metabolism. In: Scriver, C.; Beaudet, A.; Sly, W.; Valle, D., editors. The Metabolic and Molecular and Bases of Inherited Disease. 8. New York, USA: McGraw-Hill; 2001. p. 1820-1838.

Pyle JL, Kavalali ET, Piedras-Rentería ES, Tsien RW. Rapid reuse of readily releasable pool vesicles at hippocampal synapses. Neuron. 2000; 28:221–31. [PubMed: 11086996]

Rahman S, Footitt EJ, Varadkar S, Clayton PT. Inborn errors of metabolism causing epilepsy. Dev Med Child Neurol. 2013; 55:23–36.

Raux G, Bumsel E, Hecketsweiler B, van Amelsvoort T, Zinkstok J, Manouvrier-Hanu S, Fantini C, Brévière GM, Di Rosa G, Pustorino G, et al. Involvement of hyperprolinemia in cognitive and psychiatric features of the 22q11 deletion syndrome. Hum Mol Genet. 2007; 16:83–91. [PubMed: 17135275]

Robertson PL, Buchanan DN, Muenzer J. 5-Oxoprolinuria in an adolescent with chronic metabolic acidosis, mental retardation, and psychosis. J Pediatr. 1991; 118:92–5. [PubMed: 1986110]

Rocco BR, Lewis DA, Fish KN. Markedly Lower Glutamic Acid Decarboxylase 67 Protein Levels in a Subset of Boutons in Schizophrenia. Biol Psychiatry. 2016; 79:1006–15. [PubMed: 26364548]

Rodriguez-Murillo L, Gogos JA, Karayiorgou M. The genetic architecture of schizophrenia: new mutations and emerging paradigms. Annu Rev Med. 2012; 63:63–80. [PubMed: 22034867]

Roussos P, Giakoumaki SG, Bitsios P. A risk PRODH haplotype affects sensorimotor gating, memory, schizotypy, and anxiety in healthy male subjects. Biol Psychiatry. 2009; 65:1063–70. [PubMed: 19232576]

Roux F, Uhlhaas PJ. Working memory and neural oscillations: α-γ versus θ-γ codes for distinct WM information? Trends Cogn Sci. 2014; 18:16–25. [PubMed: 24268290]

Sakaba T, Neher E. Direct modulation of synaptic vesicle priming by GABA(B) receptor activation at a glutamatergic synapse. Nature. 2003; 424:775–8. [PubMed: 12917685]

Scriver CR, Whelan DT. Glutamic acid decarboxylase (GAD) in mammalian tissue outside the central nervous system, and its possible relevance to hereditary vitamin B6 dependency with seizures. Ann NY Acad Sci. 1969; 166:83–96. [PubMed: 5262035]

Sohal VS, Zhang F, Yizhar O, Deisseroth K. Parvalbumin neurons and gamma rhythms enhance cortical circuit performance. Nature. 2009; 459:698–702. [PubMed: 19396159]

Stan AD, Lewis DA. Altered cortical GABA neurotransmission in schizophrenia: insights into novel therapeutic strategies. Curr Pharm Biotechnol. 2012; 13:1557–62. [PubMed: 22283765]

Stell BM, Rostaing P, Triller A, Marty A. Activation of presynaptic GABA(A) receptors induces glutamate release from parallel fiber synapses. J Neurosci. 2007; 27:9022–31. [PubMed: 17715339]

Stevens CF, Williams JH. “Kiss and run” exocytosis at hippocampal synapses. Proc Natl Acad Sci U S A. 2000; 97:12828–33. [PubMed: 11050187]

Stork O, Ji FY, Kaneko K, Stork S, Yoshinobu Y, Moriya T, Shibata S, Obata K. Postnatal development of a GABA deficit and disturbance of neural functions in mice lacking GAD65. Brain Res. 2000; 865:45–58. [PubMed: 10814732]

Stork O, Yamanaka H, Stork S, Kume N, Obata K. Altered conditioned fear behavior in glutamate decarboxylase 65 null mutant mice. Genes Brain Behav. 2003; 2:65–70. [PubMed: 12884963]

Szabó GG, Holderith N, Gulyás AI, Freund TF, Hájos N. Distinct synaptic properties of perisomatic inhibitory cell types and their different modulation by cholinergic receptor activation in the CA3 region of the mouse hippocampus. Eur J Neurosci. 2010; 31:2234–46. [PubMed: 20529124]

Tian N, Petersen C, Kash S, Baekkeskov S, Copenhagen D, Nicoll R. The role of the synthetic enzyme GAD65 in the control of neuronal gamma-aminobutyric acid release. Proc Natl Acad Sci USA. 1999; 96:12911–6. [PubMed: 10536022]

Tomiya M, Fukushima T, Watanabe H, Fukami G, Fujisaki M, Iyo M, Hashimoto K, Mitsuhashi S, Toyo’oka T. Alterations in serum amino acid concentrations in male and female schizophrenic patients. Clin Chim Acta. 2007; 380:186–90. [PubMed: 17367771]

Uhlhaas PJ, Singer W. Abnormal neural oscillations and synchrony in schizophrenia. Nat Rev Neurosci. 2010; 11:100–13. [PubMed: 20087360]

Volman V, Behrens MM, Sejnowski TJ. Down regulation of parvalbumin at cortical GABA synapses reduces network gamma oscillatory activity. J Neurosci. 2011; 31:18137–48. [PubMed: 22159125]

Vorstman JA, Turetsky BI, Sijmens-Morcus ME, de Sain MG, Dorland B, Sprong M, Rappaport EF, Beemer FA, Emanuel BS, Kahn RS, et al. Proline affects brain function in 22q11DS children with the low activity COMT 158 allele. Neuropsychopharmacology. 2009; 34:739–46. [PubMed: 18769474]

Vreugdenhil M, Jefferys JG, Celio MR, Schwaller B. Parvalbumin-deficiency facilitates repetitive IPSCs and gamma oscillations in the hippocampus. J Neurophysiol. 2003; 89:1414–22. [PubMed: 12626620]

Wang L, Tu P, Bonet L, Aubrey KR, Supplisson S. Cytosolic transmitter concentration regulates vesicle cycling at hippocampal GABAergic terminals. Neuron. 2013; 80:143–58. [PubMed: 24094108]

Wen L, Lu YS, Zhu XH, Li XM, Woo RS, Chen YJ, Yin DM, Lai C, Terry AV Jr, Vazdarjanova A, et al. Neuregulin 1 regulates pyramidal neuron activity via ErbB4 in parvalbumin-positive interneurons. Proc Natl Acad Sci USA. 2010; 107:1211–6. [PubMed: 20080551]

Willis A, Bender HU, Steel G, Valle D. PRODH variants and risk for schizophrenia. Amino Acids. 2008; 35:673–9. [PubMed: 18528746]

Wolff SB, Gründemann J, Tovote P, Krabbe S, Jacobson GA, Müller C, Herry C, Ehrlich I, Friedrich RW, Letzkus, et al. Amygdala interneuron subtypes control fear learning through disinhibition. Nature. 2014; 509:453–8. [PubMed: 24814341]

Yang J, Chen T, Sun L, Zhao Z, Qi X, Zhou K, Cao Y, Wang X, Qiu Y, Su M, et al. Potential metabolite markers of schizophrenia. Mol Psychiatry. 2013; 18:67–78. [PubMed: 22024767]

Zarchi O, Carmel M, Avni C, Attias J, Frisch A, Michaelovsky E, Patya M, Green T, Weinberger R, Weizman A, Gothelf D. Schizophrenia-like neurophysiological abnormalities in 22q11.2 deletion syndrome and their association to COMT and PRODH genotypes. J Psychiatr Res. 2013; 47:1623–9. [PubMed: 23910792]

Zhang ZJ, Reynolds GP. A selective decrease in the relative density of parvalbumin-immunoreactive neurons in the hippocampus in schizophrenia. Schizophr Res. 2002; 55:1–10. [PubMed: 11955958]

Zucker RS, Regehr WG. Short-term synaptic plasticity. Annu Rev Physiol. 2002; 64:355–405. [PubMed: 11826273]

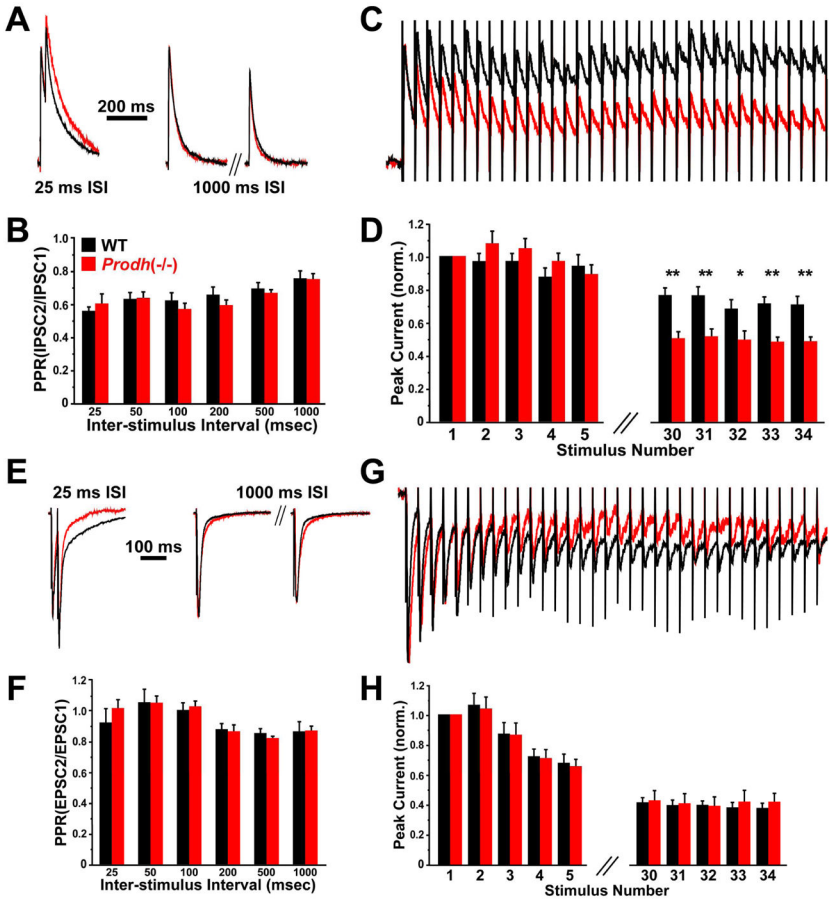

Figure 1. Sustained GABA-ergic transmission at mPFC L2/3 pyramidal cells is deficient in mice with elevated L-proline

(A) Paired-pulse ratio of IPSCs was unchanged in *Prodh*(−/−) mice (red) compared to WT mice (black). Representative traces from single recordings. Traces normalized to first response.

(B) Summary data (mean ± s.e.m.) of paired-pulse ratios of IPSCs. (WT n = 8; *Prodh*(−/−) n = 15; p > 0.25 at all tested intervals; t-test, unpaired).

(C) Synaptic depression of IPSCs during 33Hz stimulus trains was greater in *Prodh*(−/−) mice (red) versus WT mice (black). Representative traces from single recordings, normalized to first evoked response. Vertical lines, stimulus artifacts. Traces shown, 1s duration.

(D) Summary data (mean ± s.e.m.) of IPSC during 33Hz stimulus train, responses to first 5 and last 5 stimuli during a 1s stimulus train. (WT n = 11; *Prodh*(−/−) n = 10, p = 0.038, 2-way RM ANOVA; *p < 0.05, **p<0.01, Bonferroni post-hoc analysis).

(E) Paired-pulse ratio of EPSC was unchanged in *Prodh*(−/−) mice compared to WT mice.

(F) Summary data (mean ± s.e.m.) of paired-pulse ratios of EPSCs. (WT n = 8; *Prodh*(−/−) n = 6; p > 0.45 at all tested intervals; t-test, unpaired).

(G) Synaptic depression of EPSCs during 33Hz stimulus trains was unchanged in *Prodh*(−/−) mice. Normalized to first evoked response. Traces 1s in duration.

(H) Summary data (mean ± s.e.m.) of EPSC amplitudes during a 33Hz stimulus train showing response to first 5 and last 5 stimuli during 1s stimulus train. (WT n = 10; *Prodh*(−/−) n = 9, p = 0.96, 2-way RM ANOVA; p > 0.05 at all stimuli, Bonferroni post-hoc analysis).(See also Figure S1, S2).

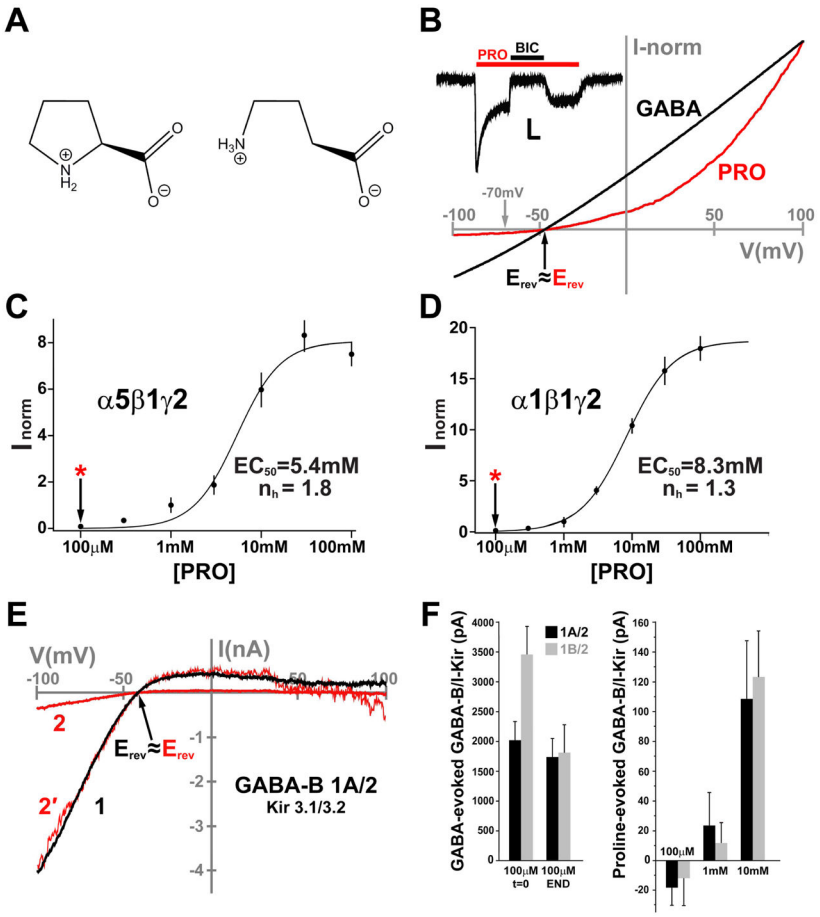

Figure 2. L-proline activates GABA-A and GABA-B receptors at supra-physiological concentrations

(A) L-proline (left) and GABA (right).

(B) Current-voltage relation for GABA (100μM, black) and L-proline (1mM, red) activation of α5β1γ2 GABA-A receptors in HEK-293 cells. Representative traces from same cell. L-proline evoked current normalized to maximal GABA-evoked current at 100mV. Inset – high dose of L-proline (30mM) evokes inward current at −90mV and is blocked by bicuculline (10μM). (Scale bar: 25pA, 5sec).

(C) Summary data (mean ± s.e.m.) of L-proline activation of α5β1γ2 GABA-A receptors at +50mV (n=8, EC_{50}=5.4, n_H=1.8). Starred arrow, maximal disease-relevant extracellular L-proline.

(D) Summary data (mean ± s.e.m.) of L-proline activation of α1β1γ2 GABA-A receptors (n=7, EC_{50}=8.3, n_H = 1.3).

(E) Current-voltage relation for GABA (100μM, black, 1) and L-proline (1mM, red, 2 and 2′) activation of Kir−3.1/3.2 currents through GABA-B 1A/2 receptors in HEK-293 cells. Representative traces from same cell. Trace 2′: L-proline evoked current normalized to maximal GABA-evoked current at −100mV.

(F) Summary data (mean ± s.e.m.) of GABA and L-proline activation of Kir−3.1/3.2 currents through GABA-B 1A/2 (black, n=8) and 1B/2 (grey, n=10) receptors. GABA-

evoked GABA-B responses before (t=0) and after (END) evaluation of L-proline responses. (See also Figure S3).

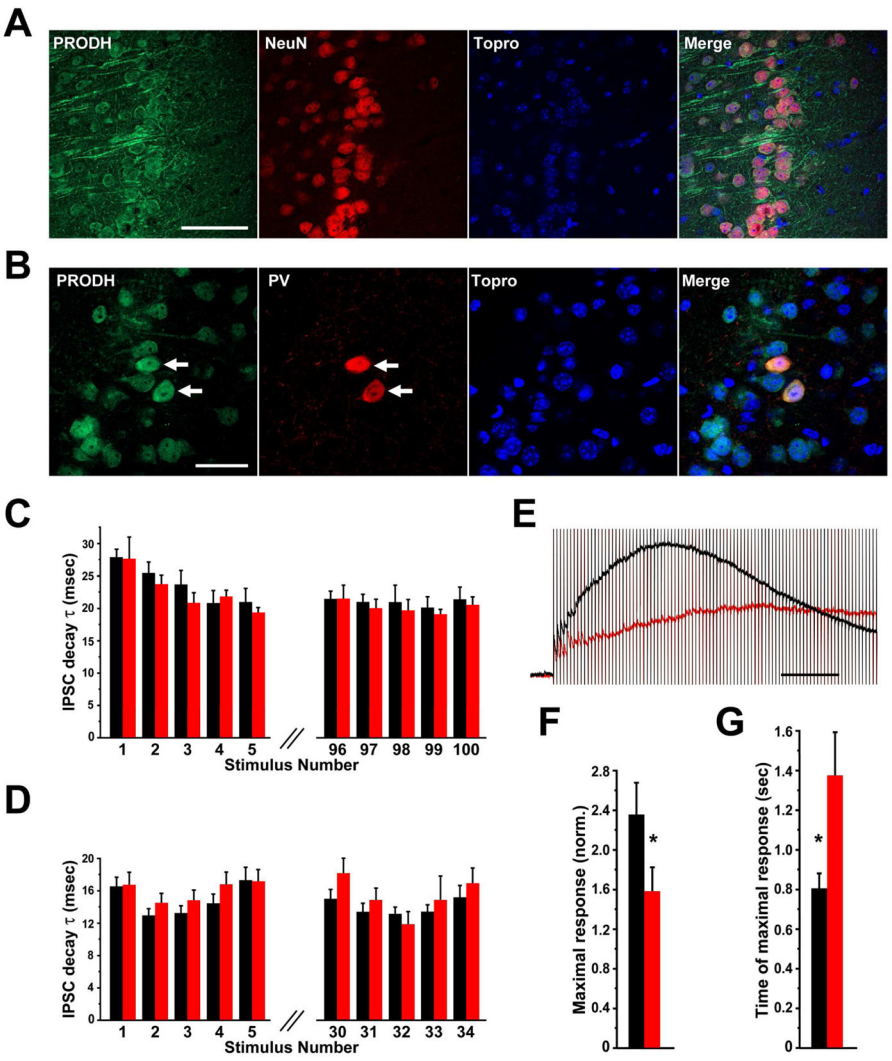

Figure 3. GABA transmission deficits in *Prodh*(−/−) mice arise presynaptically

A) WT prelimbic mPFC at L1/2 boundary showing PRODH co-localizes with neuronal marker, NeuN in a large fraction of L2/3 neurons (scale bar 100μm).

B) PRODH co-localizes with GABA-ergic marker PV in L2/3 (scale bar 50μm).

C) Summary data (mean ± s.e.m.), IPSC decay time constants (τ) during 10Hz stimulus trains unchanged in *Prodh*(−/−) mice. Analysis of recordings in Figure S2. WT, black; *Prodh*(−/−), red. (WT n = 8; *Prodh*(−/−) n = 7, p = 0.51, 2-way RM ANOVA; p > 0.05 at all stimuli, Bonferroni post-hoc analysis).

(D) Summary data, IPSC decay rate during 33Hz stimulus trains unchanged in *Prodh*(−/−) mice. Analysis of recordings in Figure 1C, 1D. (WT n = 11; *Prodh*(−/−) n = 10, p = 0.15, 2-way RM ANOVA; p > 0.05 at all stimuli, Bonferroni post-hoc analysis).

(E) Summation of IPSCs during 33Hz stimulus train in presence of GAT-1 blocker (NNC-711, 10μM) was reduced and delayed in *Prodh*(−/−). Representative traces from single recordings. Normalized to first evoked response. Scale bar 500msec.

(F) Summary data (mean ± s.e.m.), maximal IPSC summation current (normalized to first response) during 33Hz trains with GAT-1 blockade is reduced in *Prodh*(−/−) mice. (WT n = 6; *Prodh*(−/−) n = 6, p = 0.042, unpaired t-test).
(G) Summary data, latency to maximal summation during 33Hz trains with GAT-1 blockade. was delayed in *Prodh*(−/−) mice (WT n = 6; *Prodh*(−/−) n = 6, p = 0.018, unpaired t-test).
(See also Figure S4).

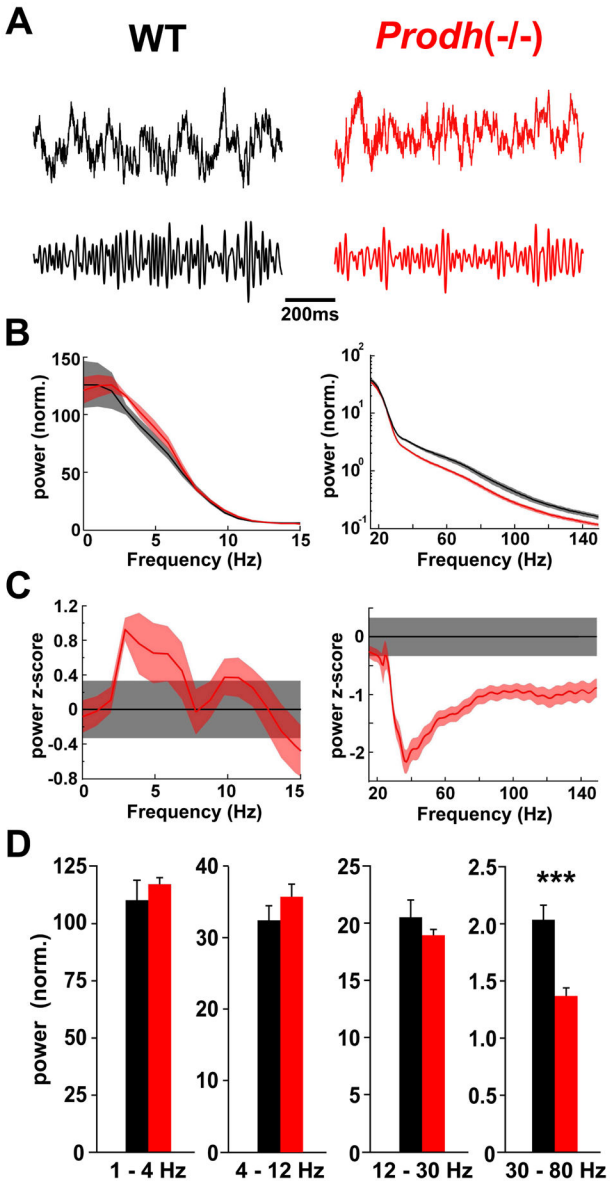

Figure 4. *Prodh*(−/−) mice exhibit gamma power deficits in mPFC

(A) Representative LFP traces from WT (left) and *Prodh*(−/−) (right) mice. Top traces, raw LFP recordings. Bottom traces, filtered 30–80Hz gamma oscillations. LFP normalized by signal root mean square.

(B) Normalized power spectra (mean ± s.e.m.) between *Prodh*(−/−) mice (n= 7, red) and WT (n = 9, black). Power spectra calculations used parameters optimized for either low (left) or high frequencies (right).

(C) Z-scored power spectra in (B) relative to WT power.

(D) Summary data (mean ± s.e.m.) of mean power across frequency ranges. WT, black; *Prodh*(−/−), red. Gamma power (30–80 Hz) was reduced in *Prodh*(−/−) mice (WT n = 9; *Prodh*(−/−) n = 7; 1 – 4 Hz: p = 0.14; 4 – 12 Hz: 0.21; 12 – 30 Hz: 0.76; 30 – 80 Hz: p = 0.000174; Wilcoxon rank-sum test, ***p < 0.001, Bonferroni-corrected).

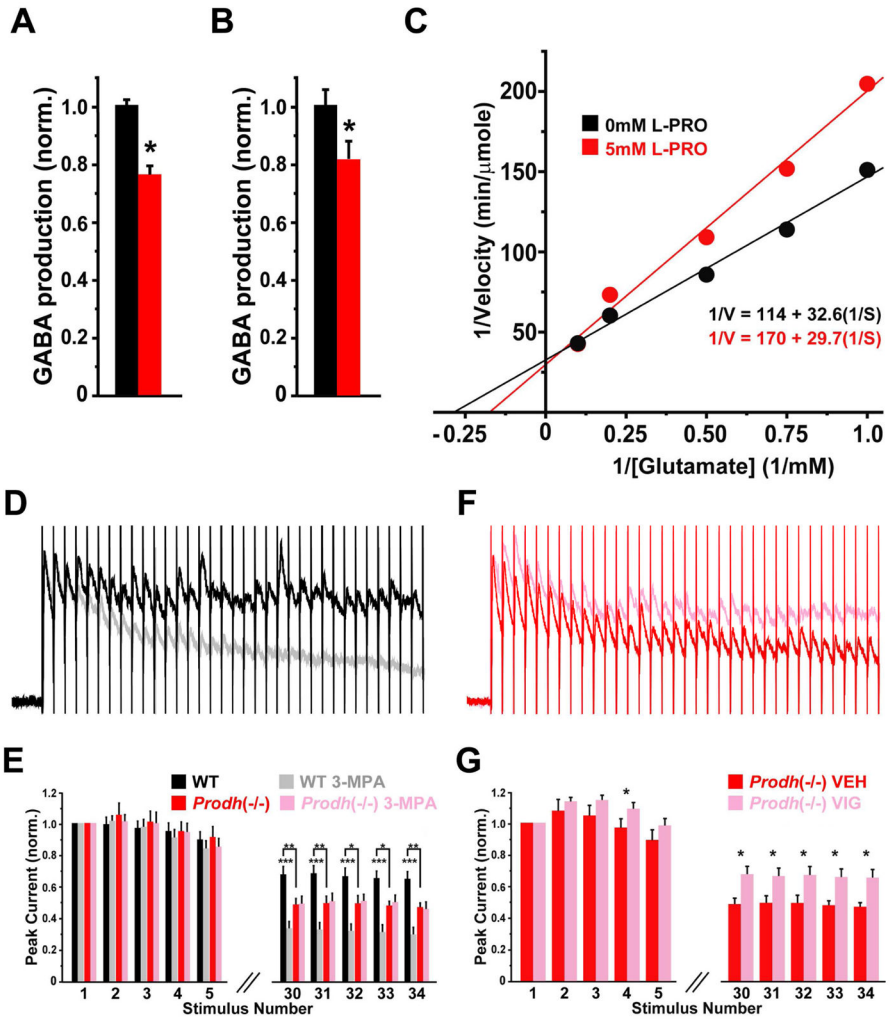

Figure 5. L-proline is a GABA-analogue that acts as a competitive inhibitor of GAD

(A) Summary data (mean ± s.e.m.), *in vitro* GABA production with recombinant human GAD67. All reactions, 5mM L-glutamate. Reactions with 1mM (black) or 5mM (red) L-proline to approximate normal and hyperprolinemic disease cytosolic L-proline levels, respectively. (1mM L-proline, n = 17, 5mM L-proline, n = 15, $p = 4.3 \times 10^{-8}$, unpaired t-test).

(B) Summary data, GABA production employing a GAD-containing cytosolic fraction from mouse PFC. * $p<0.05$. (1mM L-proline, n = 5; 5mM L-proline, n = 5, p = 0.013, unpaired t-test).

(C) Lineweaver-Burk plot of GABA production of human GAD67 comparing activity in 0mM (black, n = 5) and 5mM (red, n = 5) L-proline. Linear regression fits, solid lines and equations. Data were well fit (0mM L-proline, $R^2 = 0.990$; 5mM L-proline, $R^2 = 0.988$). Comparison of fits, p = 0.0045. Near-identical y-intercepts of linear fits indicate L-proline inhibition is competitive.

(D) Synaptic depression of IPSCs during 33Hz stimulus trains was enhanced in WT brain slices treated with the GAD blocker, 3-MPA (100μM, gray trace). Representative traces from single recordings. Normalized to the first evoked response. Traces shown, 1s in duration.

(E) Summary data (mean ± s.e.m.) of IPSC amplitudes during 33Hz stimulus train showing responses to the first 5 and last 5 stimuli during 1s stimulus train. WT, black; 3-MPA treated WT, gray; *Prodh*(−/−), red; 3-MPA treated *Prodh*(−/−), pink (WT, n = 10; WT 3-MPA, n = 11; *Prodh*(−/−), n = 12; *Prodh*(−/−) 3-MPA, n = 13. WT vs. *Prodh*(−/−) p = 0.042; WT vs. WT 3-MPA p = 0.00090; *Prodh*(−/−) vs. *Prodh*(−/−) 3-MPA p = 0.87, 2-way RM ANOVAs; *p < 0.05, **p < 0.01, ***p<0.001, Bonferroni post-hoc analysis).

(F) Enhanced synaptic depression of IPSCs during 33Hz stimulus trains in *Prodh*(−/−) slices (red trace) was reduced with a blocker of GABA degradation, vigabatrin (1500mg/kg, IP injection 2.5 days prior to recording, pink trace).

(G) Summary data, IPSC amplitudes during 33Hz stimulus train. Vehicle treated *Prodh*(−/−), red (n=10); vigabatrin treated *Prodh*(−/−), pink (n=21). (p = 0.041, 2-way RM ANOVA; *p < 0.05, Bonferroni post-hoc analysis).(See also Figures S5 and S6).